A 200 GHz Schottky Diode Quasi-Optical Detector Based on Folded Dipole Antenna

L. Liu, *Member IEEE*, H. Xu, *Member IEEE,* Y. Duan, A. W. Lichtenberger, J. L. Hesler, *Member IEEE*, and R. M. Weikle, II, *Senior Member, IEEE*

***Abstract*—We report the development of quasi-optical Schottky diode detectors based on folded dipole antennas (FDAs) having high driving point impedances. For a prototype demonstration, we have designed a 200 GHz FDA on a silicon substrate with three turns and nearly 1100 Ω input impedance. For DC signal output, we designed a coplanar strip (CPS) low-pass filter which effectively suppresses the RF (200 GHz) current on the DC lines. The detector circuits are diced into octagons for alignment with the high resistivity silicon lens. Initial responsivity and antenna pattern measurements have been performed, and the results are presented. More research will be done to further optimize the detector design and performance.**

***Index Terms*—Terahertz, quasi-optical, detector, Schottky diode, folded-dipole antenna.**

I. INTRODUCTION

TERAHERTZ detectors have a wide range of applications in spectroscopy, imaging, astronomy and bio-sensing [1-3]. Compared to other detectors such as Golay cells [4, 5] or hot-electron bolometers (HEBs) [6, 7], Schottky diode based detectors [8] have the merits of both fast response and high responsivity. In addition, they can be operated at either room or cryogenic temperature. THz waveguide or quasi-optical detectors employing zero bias Schottky diodes (ZBDs) have been developed and promising results have been reported [8, 9]. However, due to the substantial impedance mismatch between ZBDs (~1000-3000 Ω) and waveguide or antenna structures (e.g. log-periodic or sinuous antennas), the power coupling efficiency is limited, resulting in relatively low detector responsivity.

In this paper, we introduce quasi-optical Schottky diode detectors based on folded dipole antennas (FDA) having high driving point impedances. For a prototype demonstration, we have designed a 200 GHz FDA on a silicon substrate with three turns (N=3) and nearly 1200 Ω input impedance. For DC signal output, we have designed a coplanar strip (CPS) low-pass filter which effectively suppresses the RF (200 GHz) current on the DC lines. The detector circuits are diced into octagons for alignment with the high resistivity silicon lens. Initial responsivity and antenna pattern measurements have been performed, and the results are presented. On the basis of the initial testing, an anti-reflection coating will be applied to the silicon lens to reduce the coupling loss. Further research will be done to optimize the detector design and performance.

II. DETECTOR DESIGN

A. Folded Dipole Antenna

In a typical quasi-optical THz detector design, antenna structures are employed for power coupling. The input impedances of those antennas, such as annular-slot antennas and broadband self-complementary antennas on a silicon substrate, are generally less than 100 Ω. The junction resistance for a zero-bias Schottky diode, however, is in the range of 1000 to 3000 Ω. The substantial impedance mismatch between the ZBDs and antennas limits the power coupling efficiency, resulting in relatively low detector responsivity.

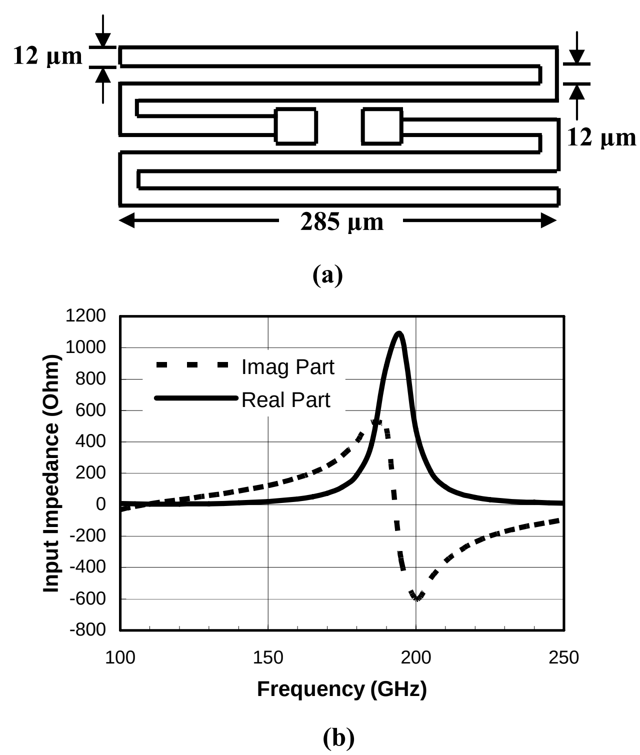

Fig. 1. Folded dipole antenna design and simulation, (a) schematic of the antenna structure for operation at 200 GHz., and (b) HFSS simulation results of the antenna input impedance.

Manuscript received 20 April 2009. This work was supported in part by the U.S. Army National Ground Intelligence Center under Grant W911W5-06-R-0001.

L. Liu. H. Xu, A. W. Lichtenberger, and R. M. Weikle, II are with the School of Engineering and Applied Science, University of Virginia, 351 McCormick Road, Charlottesville, VA 22904-4743, USA (email: ll8j@virginia.edu).

Y. Duan and J. L. Hesler are with the Virginia Diodes, Inc., 979 2nd Street NE, Suite 309, Charlottesville, VA 22903, USA.

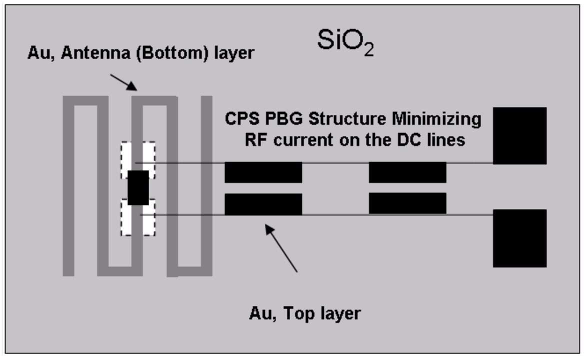

(a)

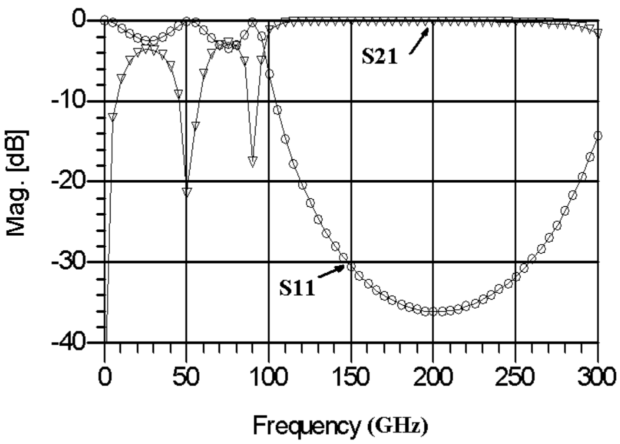

(b)

Fig. 2. (a) The overall design of the 200 GHz Schottky diode quasi-optical detector based on folded dipole antenna. The CPS PBG structure for DC signal output minimizes the RF current on the DC lines. (b) ADS Momentum simulated S parameters for the CPS low-pass filter.

A folded dipole antenna (N turns) may provide good matching characteristics for embedding ZBDs since its input impedance is determined by

$$Z_{in} = N^2 Z_0, \quad (1)$$

where Z_0 is the impedance of the ordinary single dipole [10, 11]. For a prototype demonstration, we have designed an FDA on a silicon carrier with 3 turns that operates at nearly 200 GHz. As shown in Fig. 1 (a), the length of the antenna is 285 µm. Both the antenna arm width and arm gap are 12 µm. For flip-chip mounting of the zero bias Schottky diodes, the feed point gap is 30 µm, and the contact pads dimensions are 25 µm by 25 µm. The antenna input impedance is simulated using HFSS and shown in Fig. 1 (b). The resonant frequency is 195 GHz and the real part of the impedance is nearly 1100 Ω, while the imaginary part is zero. The simulated antenna radiation patterns (both E- and H-Planes) have 3-dB beam width of around 75°.

Folded dipole antennas with *N* = 2, 3, and 4, were also simulated using HFSS, and the resonant frequency impedance increases with increasing of *N*, as expected. The antenna arm width and arm gap also affect the antenna impedance as seen from the full-wave simulation. This provides an opportunity to fine tune the antenna impedance to match that of a given ZBD junction resistance. The resulting detector will have a narrow bandwidth of nearly 20 GHz.

B. Zero Bias Schottky Diode

The zero bias Schottky diodes used in this research were fabricated at Virginia Diodes, Inc. (VDI), in a flip-chip configuration using the process described in [12]. Typical chip dimensions are 180×80×40 µm (length×width×thickness), with device parameters of I_{sat} = 11 µA, R_s = 19 Ω, ideality factor, η = 1.13, and zero bias junction resistance, dV/dI = 1-3 k Ω [8].

C. DC Output Circuit

For DC signal output, we plan to sputter 4000 Å of SiO_2 over the antenna layer for insulation, and fabricate a coplanar strip (CPS) low-pass filter (or PBG structure) which effectively suppresses the RF (200 GHz) current on the DC lines. As shown in Fig. 2 (a), the CPS LPF consists of five sections with section length of 135 µm. For the high-impedance section, the line width is 2 µm, and the gap between two lines is 80 µm, while for the low-impedance section, the line width is 43 µm, and the gap is 2 µm. The s-parameters of the CPS LPF are shown in Fig. 2 (b), and the RF suppression at around 200 GHz is as high as 36 dB. Although not designed to work as a typical LPF (large ripples in the pass band), the CPS PBG structure provides good transmission for DC and very low frequency signals.

III. Detector Fabrication and Assembly

The detector circuits were fabricated in the Microfabrication Laboratory at the University of Virginia (UVML). For a prototype demonstration, folded dipole antennas with three turns that operate at nearly 200 GHz were fabricated on 0.5mm-thick high-resistivity (≥ 20000 Ω·cm) silicon wafer (ε_r = 11.8), using a traditional Au plating process. The antennas are connected to DC output pads using two meander lines (2 µm width) at both ends (see Fig. 3 (b)). In principle, the radiation due to RF currents on each of the meander lines cancel each other in the far field, thus reducing their influence on the folded dipole antennas.

The antenna will be mounted on an extended hemispherical high-resistivity (≥1000 Ω·cm) silicon lens (ε_r = 11.8) with radius *R*, of 5 mm. The total extension length (*L*) is chosen to be 1 mm (*L*/*R* ~ 0.2) for high Gaussian coupling efficiency. According to [13], most of the power is radiated into the dielectric side, and the use of a silicon substrate with high dielectric constant further enhances the power coupling efficiency for a receiving antenna. In addition, using the same material for both the substrate and lens eliminates the power loss to substrate modes [14].

As shown in Fig. 3, a quasi-optical detector mount has been employed for coupling the input power to the folded dipole antenna. The detector chips have been diced into octagons for alignment with the high-resistivity silicon lens. The zero bias Schottky diode is mounted at the center of the antenna using flip-chip mounting technique (see inset of Fig. 3 (b)). The

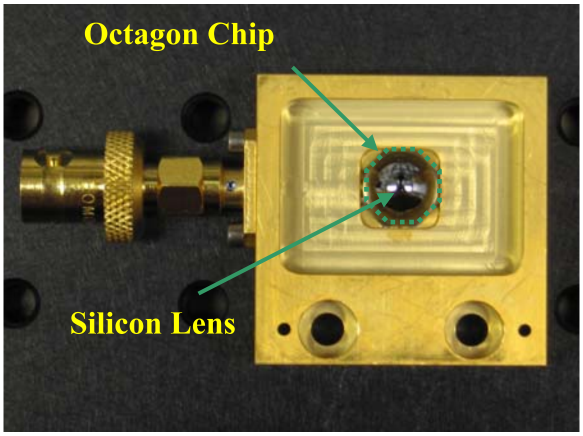

(a)

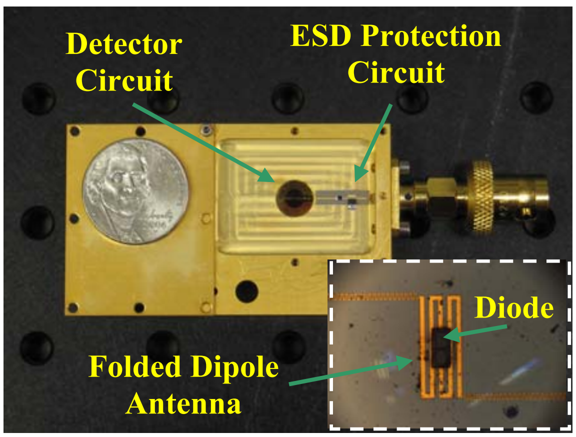

(b)

Fig. 3. The circuits and quasi-optical block of the 200 GHz folded dipole antenna detector. (a) The front-side view of the quasi-optical detector block with extended hemispherical silicon lens. (b) The back-side view of the detector with ESD protection circuit. The inset shows the folded dipole antenna with a flip-chip mounted ZBD and meander lines.

detector circuit is mounted on the back side of the block, and a high-resistivity silicon lens (R = 5 mm) is attached against the detector chip from the front side. An ESD protection circuit is also mounted and all connections are accomplished using wire-bonding techniques.

IV. Measurements

A. Detector Responsivity Measurement

The detector responsivity measurement setup is shown in Fig. 4. An Agilent microwave source together with a VDI 140-240 GHz FEM are employed to provide the THz radiation through a diagonal horn antenna. In between the VDI FEM and the horn antenna, a waveguide directional coupler is inserted to monitor the output power with an Ericson power meter. Two off-axis parabolic mirrors (f = 76.4 mm) are utilized to couple the THz radiation onto the ZBD folded dipole detector. The THz radiation is modulated with a chopper at 100 Hz, and the DC output signal from the detector is measured using a lock-in amplifier.

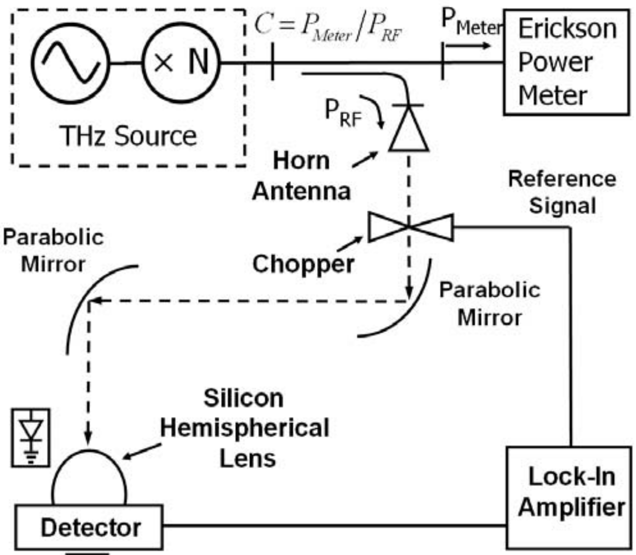

Fig. 4. The detector responsivity measurement setup for the frequency range of 140 GHz to 240 GHz. Two parabolic mirrors are utilized for coupling the RF power onto the detector. The DC output signal is modulated at 100 Hz and measured with a lock-in amplifier.

Fig. 5(a) shows the results for detector responsivity measurement at 140 to 240 GHz. A peak responsivity of around 280 V/W (without any corrections) is observed at 186 GHz. Compared to the designed working frequency of 195 GHz, the measured resonant frequency is shifted to a lower frequency. This might be a result of loading due to the meander lines at both of the antenna arm ends, which effectively increases the antenna electrical length. The detector responsivity decreases rapidly from the center frequency (186 GHz), and drops to below 100 V/W at 140 GHz, and is lower than 15 V/W at 240 GHz, showing the anticipated narrow bandwidth of this detector. The estimated bandwidth is approximately 20 GHz, which is close to the simulation results. The corresponding NEP is ~20 pW/√Hz at the resonant frequency, according to [8]. However, the peak responsivity of 280 V/W is much lower than what we expected, and analysis and discussion of this will be presented in section V.

B. Antenna Characterization

To ensure that the designed folded dipole antenna is working properly, the far-field radiation patterns of the antenna on an extended hemispherical silicon lens have been measured at ~190 GHz. In this measurement, VDI frequency extension modules (FEMs) cover the frequency range of 190 GHz to 210 GHz, were utilized for providing the THz radiation. The detector was mounted on a computer-controlled rotation stage and the output DC signal was modulated and detected by a lock-in amplifier. As shown in Fig. 5 (b), the measured radiation patterns show reasonable Gaussian-shape main beams with side-lobe level less than -14 dB. The 3-dB beam width of the folded dipole antenna is 10° at 190 GHz. The measured H-plane radiation pattern is slightly broader than the pattern in the E-plane, as expected, according to [13].

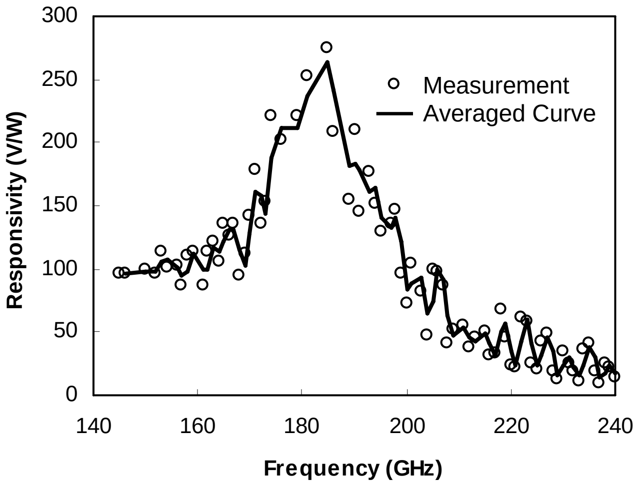

(a)

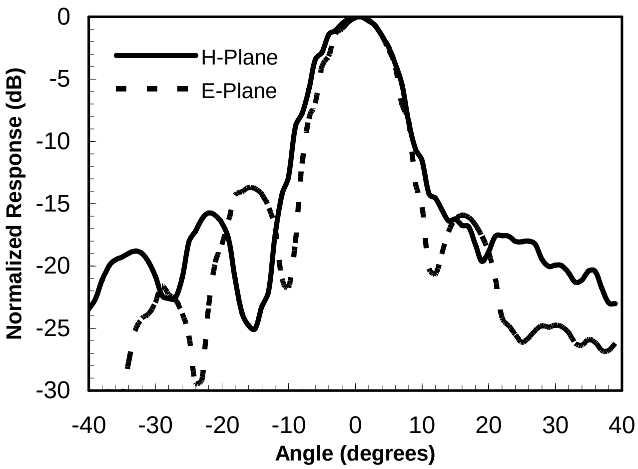

(b)

Fig. 5. Detector initial measurement results: (a) responsivity measurement in the frequency range of 140-240 GHz. A peak responsivity of ~280 V/W is observed at 186 GHz, (b) antenna radiation patterns measured at 190 GHz show good Gaussian-shape main beams.

V. Discussion and Comparison

To evaluate the performance of this quasi-optical Schottky diode detector based on the folded dipole antenna, we compare its responsivity to two different detectors. Using the same experimental setup as shown in Fig. 4, we measured the responsivity of a WR-5 waveguide detector with horn antenna, and a broadband quasi-optical detector (planar sinuous antenna) developed by our group in [9], in the frequency range of 140-240 GHz. The results are summarized in Fig. 6. The waveguide detector has a typical responsivity of 600-1200 V/W over the entire WR-5 frequency band, with good performance (~200 V/W) up to 230 GHz. The broadband quasi-optical detector exhibited a responsivity of 200-800 V/W over the entire frequency range. Its performance is slightly better than the waveguide version at frequencies higher than 210 GHz, demonstrating its broadband property. The folded dipole Schottky diode detector, however, shows a relatively low peak responsivity at 186 GHz.

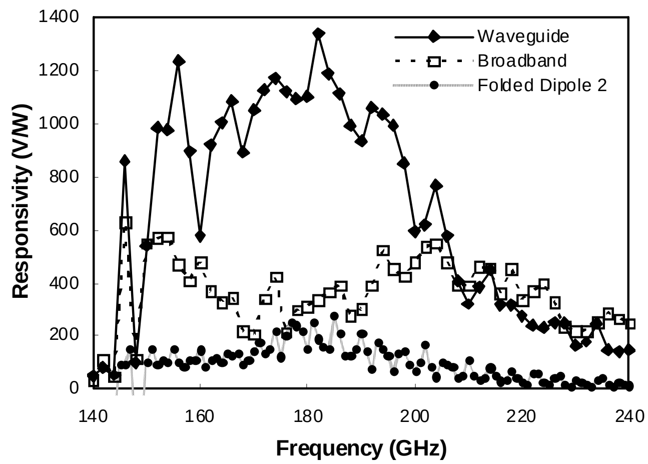

Fig. 6. Responsivity measurement of three different zero bias Schottky diode detectors comparing their performance in the frequency range of 140-240 GHz.

Although the antenna is working more-or-less as designed (as seen in Fig. 5), the center frequency responsivity is much lower than expected. With impedance matching between the antenna and ZBD, RF power reflection of up to nearly 80% are avoided, and a responsivity of 600-1500 V/W (3-5 times better than the broadband version), at resonant frequency, is expected. Since this detector is designed for narrow band applications, the goal responsivity of 1000-2500 V/W (quasi-optically) can be achieved, in principle, by applying anti-reflection coating to the silicon lens. We attribute the measured low responsivity to the following several factors: 1. the fabricated circuit is a simplified version (with meander lines for DC output) for quick diagnostics; 2. the Schottky diode chip is much larger than the designed contact pads for flip-chip mounting (see Fig. 3(b)), which effectively loads a metal layer (Au) and a dielectric (GaAs, $\varepsilon_r = 10.9$) layer at the antenna feed point, resulting in a different drive point impedance and resonant frequency; 3. the responsivity measurement system is not optimized.

On the basis of the above discussion, we plan to further simulate the fabricated detector structure with the loading of the metal and dielectric layers at the antenna feed point to understand its effect to the detector performance. Meanwhile, we will continue to fabricate the detector circuit described in Fig. 2, and measure the performance with an optimized experimental setup.

Acknowledgment

The authors would like to thank all the colleagues from the UVML, the Microwave Laboratory, and the FIR-THz Laboratory at the University of Virginia. The authors are also grateful for the assistance and advice of Professors Acar Isın and Bascom S. Deaver, Jr., both with the Department of Physics at the University of Virginia, Charlottesville, VA.

REFERENCES

[1] P. H. Seigel, "Terahertz technology," *IEEE Trans. Microwave Theory and Tech*., vol. 50, no. 3, pp. 910–928, March 2002.

[2] B. H. Deng, C. W. Domier, and N. C. Luhmann, Jr. *et al*., "ECE imaging of electron temperature and electron fluctuations," *Rev. Sci. Instrum.*, vol. 72, no. 1, pp. 301–306, Jan. 2001.

[3] D. Woolard *et al*., "The potential use of submillimeter-wave spectroscopy as a technique for biological warfare agent detection," *22nd Army Sci. Conf.*, Baltimore, MD, Dec. 12–13, 2000.

[4] P. R. Griffiths and J. A. de Haseth, "Fourier transform infrared spectrometry," *Wiley Interscience*, New York, pp. 209–212, 1986.

[5] P. R. Griffiths and C. C. Homes, "Instrumentation for far-infrared spectroscopy," *Handbook of Vibrational Spectroscopy*, vol 1–Theory and Instrumentation, Wiley, New York, 2001.

[6] J. Wei, D. Olaya, B. S. Karasik, S. V. Pereverzev, A. V. Sergeev, and M. E. Gershenson, "Ultrasensitive hot-electron nanobolometers for terahertz astrophysics," *Nature Nanotech.*, no. 3, pp. 496-500, July 2008.

[7] L. Liu, H. Xu, R. R. Percy, D. L. Herald, A. W. Lichtenberger, J. L. Hesler, and R. M. Weikle, "Development of integrated terahertz broadband detectors utilizing superconducting hot-electron bolometers," *IEEE Trans. Appl. Supercon.*, to be published, Jun. 2009.

[8] J. L. Hesler, and T. W. Crowe, "Responsivity and noise measurements of zero-bias Schottky diode detectors," *18th Intl. Symp. Space Terahertz Techn.*, Pasadena, March 2007.

[9] J. L. Hesler, L. Liu, H. Xu, and R. M. Weikle, II, "The development of quasi-optical THz detectors," *33rd International Conference on Infrared, Millimeter, and Terahertz Waves (IRMMW)*, Pasadena, California, USA, Sep. 2008.

[10] C. A. Balanis, "Antenna theory: analysis and design," 2nd Edition, *John Wiley & Sons, Inc.*, 1997.

[11] H. C. Ryu, S. I. Kim, M. H. Kwak, K. Y. Kang, and S. O. Park, "A folded dipole antenna having extremely high input impedance for continuous-wave terahertz power enhancement," *33rd International Conference on Infrared, Millimeter, and Terahertz Waves (IRMMW)*, Pasadena, California, USA, Sep. 2008.

[12] W. L. Bishop, E. Meiburg, R. J. Mattauch, T. W. Crowe and L. Poli, "A micron-thickness, planar Schottky diode chip for terahertz applications with theoretical minimum parasitic capacitance," *IEEE MTT-S Int. Micwave Symp. Digest*, pp. 1305–1308, May 1990. *r Quantities*, ANSI Standard Y10.5-1968.

[13] D. F. Filipovic, S. S. Gearhart, and G. M. Rebeiz, "Double slot antennas on extended hemispherical and elliptical silicon dielectric lenses," *IEEE Trans. Microwave Theory & Tech.*, vol. 41, pp. 1738-1749, Oct. 1991.

[14] D. B. Rutledge, and M. S. Muha, "Imaging antenna arrays," *IEEE Trans. Antennas Propagat.*, vol. AP-30, no. 4, pp. 535-540, July 1982.